ARTICLE

pubs.acs.org/est

Nitrogen-Containing Organic Compounds and Oligomers in Secondary Organic Aerosol Formed by Photooxidation of Isoprene

Tran B. Nguyen

Department of Chemistry, University of California, Irvine, California 92697, United States

Julia Laskin

Chemical and Materials Sciences Division, Pacific Northwest National Laboratory, Richland, Washington 99352, United States

Alexander Laskin

Environmental Molecular Sciences Laboratory, Pacific Northwest National Laboratory, Richland, Washington 99352, United States

Sergey A. Nizkorodov*

Department of Chemistry, University of California, Irvine, California 92697, United States

Supporting Information

ABSTRACT: Electrospray ionization high-resolution mass spectrometry (ESI HR-MS) was used to probe molecular structures of oligomers in secondary organic aerosol (SOA) generated in laboratory experiments on isoprene photooxidation at low- and high-NO_x conditions. Approximately 80−90% of the observed products are oligomers and up to 33% by number are nitrogen-containing organic compounds (NOC). We observe oligomers with maximum 8 monomer units in length. Tandem mass spectrometry (MS^n) confirms NOC compounds are organic nitrates and elucidates plausible chemical building blocks contributing to oligomer formation. Most organic nitrates are comprised of methylglyceric acid units. Other important multifunctional C_2−C_5 monomer units are identified including methylglyoxal, hydroxyacetone, hydroxyacetic acid, and glycolaldehyde. Although the molar fraction of NOC in the high-NO_x SOA is high, the majority of the NOC oligomers contain only one nitrate moiety resulting in a low average N:C ratio of 0.019. Average O:C ratios of the detected SOA compounds are 0.54 under the low-NO_x conditions and 0.83 under the high-NO_x conditions. Our results underscore the importance of isoprene photooxidation as a source of NOC in organic particulate matter.

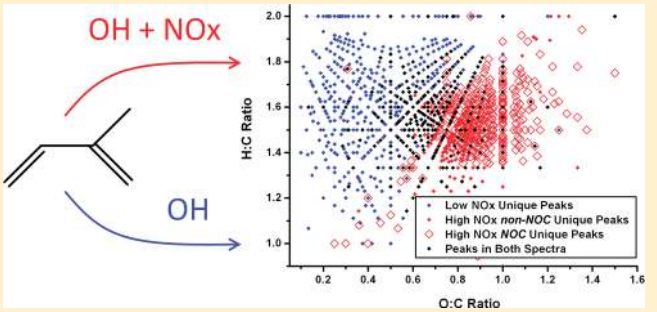

1. INTRODUCTION

Isoprene (2-methyl-1,3-butadiene, C_5H_8), the most abundant nonmethane hydrocarbon in the atmosphere,[1] is a major precursor to secondary organic aerosol (SOA).[2−4] Photooxidation of isoprene produces a number of compounds that end up in SOA, including tracer molecules 2-methylglyceric acid (2MGA) and 2-methyltetrols.[5−10] Oligomer formation by particle-phase accretion reactions is significant in isoprene SOA.[11,12]

The initial concentrations of nitrogen oxides ($NO + NO_2 = NO_x$) in chamber photooxidation experiments affects the semivolatile and nonvolatile products produced from isoprene and, therefore, the yield and composition of the SOA.[8,13−15] Under high-NO_x conditions, relevant to urban environments, the chemistry of alkylperoxy radicals (RO_2) is controlled by the $RO_2 + NO \rightarrow RO + NO_2$ reaction, and favors production of carbonyl compounds in the gas phase.[16] Furthermore, under high-NO_x conditions, the yield of gas-phase organic nitrates from isoprene is significant, in the range of 8−13%.[17−19] As these organic nitrates are expected to be large (C_4−C_5) and bifunctional,[20] they can enter the particle phase through gas/particle partitioning, reactive uptake, and oligomerization. In contrast, under low-NO_x conditions, relevant to more pristine environments like the Amazon basin, the $RO_2 + HO_2 \rightarrow ROOH + O_2$ reaction becomes the dominant fate of RO_2 radicals, and organic nitrates are expected to have negligible yields.

The SOA yield from the photooxidation of isoprene has been extensively investigated in laboratory chamber studies over a broad range of NO_x concentrations.[21] However, the particle-phase

Received: May 11, 2011
Accepted: July 6, 2011
Revised: June 29, 2011
Published: July 06, 2011

composition has not been studied in detail until the work of Surratt et al. (2006).[8] That study identified ~22−34% of the high-NO_x aerosol mass as oligomers and suggested 2MGA to be a key monomer unit forming oligomers by esterification reactions. (Herein, we use the terms oligomers and high-MW compounds interchangeably for constituents of isoprene SOA with molecular weights in excess of 200 g/mol, which corresponds to at least two monomeric products bound together.) Gas chromatography ion-trap MS studies by Szmigielski et al. (2007) identified 2MGA as a prominent oligomer building block.[22] In addition, the nitrogen-containing organic compounds (NOC) in isoprene SOA formed under high-NO_x were shown to be organic mononitrates. A recent study of the photooxidation of methacrolein further confirmed 2MGA as a key monomer in SOA oligomerization reactions.[23] The overall conclusion from these studies is that more acidic products are formed under high-NO_x conditions with a greater contribution from dihydroxyacids like 2MGA. However, a large fraction of the oligomeric compounds remains uncharacterized because the highly diverse nature of oligomer building blocks in isoprene SOA complicates the molecular level analysis.

In this work, we use electrospray ionization high-resolution mass spectrometry (ESI HR-MS) to overcome this limitation and provide additional insights into the compositional differences, which control the physical and chemical properties of SOA formed under the high- and low-NO_x oxidation regimes. An emphasis is placed on the organic nitrate fraction (both mono- and poly nitrates), comparing the sample-averaged elemental ratios (H:C, O:C, and N:C ratios) of the detected SOA compounds, and studying a large pool of oligomer building blocks in low-NO_x and high-NO_x SOA generated from the photooxidation of isoprene.

2. EXPERIMENTAL SECTION

Photooxidation of isoprene was performed in a 5 m^3 Teflon chamber under dry (RH < 2%) conditions in the absence of seed particles. For all experiments, the chamber was flushed overnight with dried air from an FTIR purge gas generator (Parker model 75−62). Reagents were added to the chamber by evaporation of 40 μL of H_2O_2 (Aldrich, 30% by volume in water) with a stream of air, followed by injection of 5 μL isoprene (Aldrich, 99% purity). For high-NO_x experiments, NO was introduced by adding a calibrated volume of a primary standard (Praxair, 5000 ppm NO in N_2) into the chamber. Some NO_2 was usually produced when the NO standard was injected in the chamber. A fan mixed the reagents within the chamber for several minutes and was then turned off to minimize particle wall losses. In all experiments, the starting mixing ratios of isoprene and H_2O_2 were 250 ppb and 2 ppm, respectively. For high-NO_x experiments, the initial mixing ratios of NO and NO_2 were 600 and 100 ppb, respectively. For low-NO_x experiments, the initial mixing ratios of NO and NO_2 were <1 ppb and <3 ppb, respectively. Supporting Information (SI) Figure S1 shows that in the high-NO_x oxidation, NO decreased to below the detection limit after approximately 40 min. In the low-NO_x oxidation, NO decreased quickly and remained below the detection limit throughout the oxidation period. After the concentrations of all reagents stabilized, UV-B lamps, with emission centered at 310 nm, were turned on to initiate the photochemistry. The photooxidation time was two hours.

The formation of SOA particles was monitored by a scanning mobility particle sizer (SMPS model 3080, TSI Inc.), ozone was monitored by a Thermo model 49i photometer, NO and NO_y were measured with Thermo model 42i chemiluminescence analyzer. A proton-transfer-reaction time-of-flight mass spectrometer (PTR-ToF-MS, Ionicon Analytik) was used to follow the decay of isoprene and the production of the gas-phase photooxidation products. The PTR-ToF-MS was operated with a resolving power (ratio of the peak position to its full width at half-maximum) of around 1500 at m/z 69 (the nominal mass of the protonated isoprene). Calibration was performed for certain groups of compounds for the purpose of estimating their gas-phase concentrations: alcohols (methanol and pentanol), aldehydes (formaldehyde), ketones (acetone and cyclohexanone), and alkenes (isoprene and pinene). Not all VOC, especially multifunctional compounds, are available as standards for calibration. For quantification of such compounds we assumed a PTR rate constant of 2×10^{-9} cm^3 s^{-1} $molec^{-1}$. The concentrations measured with PTR-ToF-MS for the uncalibrated VOC may be off by a factor of ~3 as the PTR rate constants for oxygenated VOC typically range from 1×10^{-9} to 5×10^{-9} cm^3 s^{-1} $molec^{-1}$.[24] The difference in SOA yield, production of VOC and decay of isoprene observed using PTR-ToF-MS is in good agreement with previous accounts of isoprene gas-phase oxidation and are shown in Figures S1 and S2 of the SI section. The OH concentration was higher in the high-NO_x photooxidation due to OH recycling from $NO + HO_2 \rightarrow OH + NO_2$ reaction.[16] The initial OH concentration was estimated from the decay rate of isoprene, and it was 2×10^7 and 4×10^7 molecules cm^{-3} under the low-NO_x and high-NO_x conditions, respectively. Figure S1 in the SI shows the time-dependence of NO, O_3, SOA yield, and selected VOC mixing ratios in the chamber. The higher OH concentration at high-NO_x conditions leads to a faster decay of isoprene and its first-generation products resulting in correspondingly higher SOA yields. Based on the PTR-ToF-MS time profile of the reactions, we expect a higher contribution of second-generation oxidation products in the high-NO_x oxidation SOA.

In the high-NO_x reaction, the concentration of O_3 starts to build up after a large fraction of isoprene is consumed. Based on the reaction rates of the first generation products, for example, methyl vinyl ketone (MVK), with O_3[25] and OH,[26] and the estimated concentrations of OH and O_3 in our chamber, the maximum contribution of the O_3-initiated chemistry to the total product formation is ca. 10%. From structure-based volatility estimations,[27] the O_3 + isoprene products are expected to be more volatile than OH + isoprene products. Therefore, the contribution of O_3 + isoprene to the particle-phase fraction is predicted to be minor under the present experimental conditions. The contribution of NO_3 to the oxidation of isoprene is also expected to be minor because its concentration is strongly suppressed by photolysis. Furthermore, NO_3-initiated oxidation is expected to produce more polynitrates and result in a higher SOA compared to what we observe in this study.[28] However, as NO_3 concentration increases after the lights are off, it may still contribute to aging of aerosol during collection of particles from the dark chamber.

The SOA loadings after two hours of reaction were 20 and 40 $\mu g/m^3$, under the low-NO_x and high-NO_x conditions, respectively. Aerosols were collected onto Teflon filter substrates (Millipore 0.2 μm pore size) using a multistage micro-orifice uniform deposition impactor (MOUDI) operated at 30 standard liters per minute. The collection lasted for 3 h, which allowed oligomerization reactions to continue in the dark. Collected samples were placed in plastic holders, vacuum-sealed in polyethylene bags, and frozen at −20 °C pending offline analysis that took place several days after collection. Blank samples were generated under the same experimental conditions,

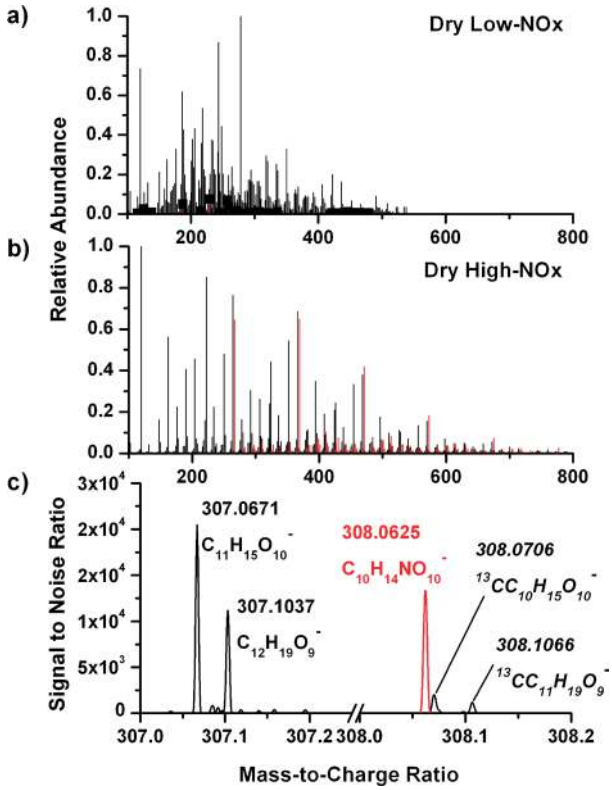

Figure 1. Representative high-resolution (−) ESI mass spectra of SOA obtained from photooxidation of isoprene under dry conditions in the (a) low- and (b) high-NO_x experiments. NOC peaks are shown in red. Panel (c) is a magnified view of the high-NO_x mass spectrum, illustrating the unambiguous resolution of peaks belonging to nitrogen-containing molecules and those of ^{13}C satellites around m/z 308.

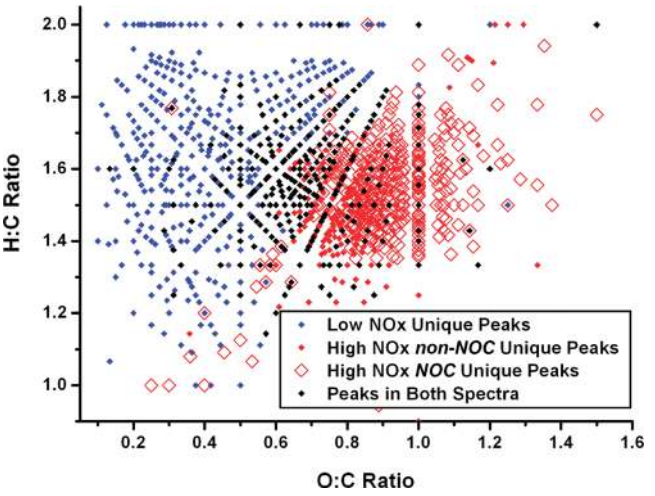

Figure 2. Van Krevelen diagram of SOA obtained from photooxidation of isoprene. Peaks corresponding to NOC observed in the high-NO_x spectra are shown with open red markers. Filled markers correspond to nitrogen-free products observed either uniquely under low-NO_x (blue) and high-NO_x (red) conditions or under both conditions (black). Intensity weighted average elemental ratios were determined as: O:C = 0.54, H:C = 1.61, N:C < 0.002 for low-NO_x SOA, and O:C = 0.83, H:C = 1.55, N:C = 0.019 for high-NO_x SOA.

but in the absence of the UV radiation. Particle mass concentrations in the background (before isoprene was injected) and in the blank samples (2 h of VOC + H_2O_2 sitting in the chamber in darkness) were both <0.01 $\mu g/m^3$.

The SOA samples were analyzed using a high-resolution linear ion trap (LTQ-) Orbitrap mass spectrometer (Thermo, inc.) equipped with a modified electrospray ionization (ESI) source with a fused silica capillary (50 μm ID) spray tip. SOA samples were extracted with 10 min sonication in a mixture (1:1 v/v) of acetonitrile and water (both Acros Organics, HPLC grade). The estimated SOA material concentration after the extraction was ~100 μg/mL. The mass spectrometer was operated in the negative ion mode, with analyte molecules being detected as $[M-H]^-$ in the mass range of m/z 50−2000. The spray voltage was 4 kV and the solvent flow rate was 0.5 μL/min. Background mass spectra were taken on filters obtained from blank experiments. The mass resolving power of the instrument was 60,000 at m/z 400. Mass calibrations with a commercial standard mixture of caffeine, MRFA, and Ultramark 1621 (MSCAL5, Aldrich) were performed in intervals of several hours to conserve mass accuracy (0.5 ppm at m/z 500).

Data analysis on all samples was performed in a similar manner to our previous works.[29,30] All mass spectra were processed to exclude peaks present in the spectra obtained from blank experiments (no UV). The peaks were assigned elemental formulas $C_cH_hO_oN_n$, using valence, parity, atomic ratio, and isotopic constraints. Because deprotonation was assumed to be the major ionization mechanism, formulas of neutral SOA compounds were obtained by adding one hydrogen atom to the ionic formulas. Typically >1000 distinct peaks were detected in the SOA samples and 60−70% peaks were unambiguously assigned to a molecular formula. The unassigned peaks were low in ion abundance with the signal-to-noise <1% of the main peak.

3. RESULTS AND DISCUSSION

3.1. Mass Spectra and Elemental Ratios. Figure 1a and b show characteristic high-resolution negative ion mode ESI mass spectra for isoprene photooxidation SOA, with NOC peaks marked in red. Approximately 700 compounds were assigned for the low-NO_x sample and 900 compounds were assigned for the high-NO_x sample. 80−90% of detected peaks corresponded to high-MW compounds (>200 Da), which is significantly higher than 22−34% reported by Surratt et al. (2006).[8] In our work, high-MW compounds may be overestimated because they tend to be ionized with higher efficiency relative to low-MW compounds. In contrast, in the work of Surratt et al. (2006), high-MW oligomers may hydrolyze during the chromatographic separation. Therefore, one should view the 80−90% value reported in our study as an upper limit and the 22−34% value reported in the Surratt et al. (2006) study as a lower limit for the actual oligomeric content.

In this work, ions $C_cH_{h-1}O_oN_n^-$ and the corresponding neutrals $C_cH_hO_oN_n$ with $n > 0$ are referred to as NOC. Mass spectra of SOA generated under two NO_x conditions are clearly different from each other. In the low-NO_x sample, the mass range of observed molecules is approximately m/z 80−600, which is consistent with MALDI-MS observations of Surratt et al. (2006), and the spectrum is dominated by dimer and trimer peaks clustered around m/z 200. Peaks with even nominal masses have relatively small intensities suggesting that most ions have no nitrogen atoms in them. The corresponding carbon numbers of the compounds range from C_2 to C_{29}.

In contrast, the high-NO_x mass spectrum spans a wider range of masses indicating more extensive oligomerization under these conditions. The mass range of observed molecules is m/z 80−900, again consistent with ESI-MS observations of Surratt et al. (2006), with corresponding carbon numbers of C_2−C_{35}. A number of abundant peaks in the spectrum have even nominal masses characteristic of molecules containing an odd number of nitrogen atoms. The mass resolving power of the Orbitrap is sufficient to resolve the NOC peaks from the ^{13}C satellite peaks at the same nominal mass (Figure 1c). The mass difference between ^{13}C and N is 0.008 Da, and the peak width at half-maximum is 0.005 Da at m/z 300. Even though the NOC and ^{13}C peaks start to merge above m/z 500, we can still confidently assign the NOC peaks in cases when the peak intensities exceed those predicted from the natural abundance of ^{13}C.

Figure 2 is a graphical representation of the degree of alkylation and oxidation of the isoprene SOA formed in the low-NO_x vs high-NO_x samples in the form of a Van Krevelen (VK) diagram,[31,32] where the H:C ratios of the individual SOA compounds are plotted against the O:C ratios. Elemental ratios shown in Figure 2 are those of individual molecules that were assigned based on HR-MS analysis. Each point on the VK diagram may represent more than one molecule because a number of observed SOA compounds have the same combination of H:C and O:C ratios. The low-NO_x and high-NO_x data were separated into three categories: peaks observed in both data sets, peaks observed uniquely in the low-NO_x data, and peaks observed uniquely in the high-NO_x data. Compounds observed under both conditions span a broad range of the O:C and H:C ratios. In contrast, the elemental ratios of compounds unique to the low-NO_x SOA sample are clustered around the low O:C ratio region and those of the high-NO_x SOA compounds tend to have higher O:C values. The intensity-weighted average O:C ratios of the detectable compounds, calculated in an identical manner to our previous work,[29] are 0.54 and 0.83 under low-NO_x and high-NO_x conditions, respectively. The higher average O:C in the high-NO_x experiments is attributed to more extensive oxidation in the gas-phase (the OH concentrations are higher by at least a factor of 2 compared to the low-NO_x experiments) and higher incorporation of organic nitrates in the particles, as we will discuss in Section 3.2. Each $-ONO_2$ group contributes three oxygen atoms to the molecular formula, thus resulting in higher O:C values.

How do the O:C ratios determined in this work compare with the existing field and laboratory measurements reported by aerosol mass spectrometry (AMS) methods?[33] One caveat in making such comparisons is bias toward preferential detection of oxygenated organic and organic nitrate species in the ESI negative ion mode, which may lead to an overestimation of the actual O:C value. However, the disparity of O:C values obtained in positive vs negative ion mode ESI is not expected to be large. For example, the O:C values measured for ozone-isoprene SOA in the positive and negative ion mode ESI[29] were 0.61 and 0.63, respectively. The O:C and N:C ratios quantified by AMS are affected by the opposite problem: they may underestimate the true values.[34,35] Despite these limitations, the low-NO_x O:C ratio of 0.54 obtained in this study compares favorably to the AMS O:C values of 0.41−0.77 measured in chamber studies[34] and 0.39−0.45 measured in low-sulfate aerosol particles in the Amazon basin.[36] The lower O:C ratio obtained in the field experiments may be attributed to the contribution from monoterpene oxidation products. For example, the average O:C values

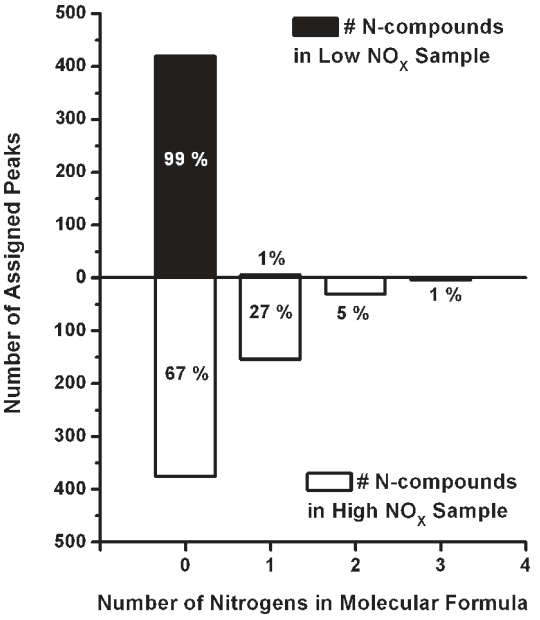

Figure 3. The distribution of NOC compounds in SOA generated from the low- and high-NO_x photooxidation of isoprene. Most particle-phase compounds do not contain nitrogen even when generated under high initial NO_x concentrations; however, a significant fraction of high-NO_x SOA molecules contain one (27%), two (5%), and three (1%) nitrogen atoms.

are lower for alpha-pinene ozonolysis and photooxidation SOA (0.29−0.45)[37−39] and for limonene ozonolysis SOA (0.43−0.50).[40,41]

The O:C ratio of the high-NO_x SOA may be compared to those from aerosols sampled in forested sites affected by urban NO_x emissions, e.g. Whistler Mountain, Canada, which is close to major highways. The high-NO_x O:C value of 0.83 obtained in this study compares well with the O:C range of 0.43−0.81 obtained in chamber studies[34] and value of 0.83 measured on the Whistler Mountains in Canada.[42] A comparison to a predominantly urban site can also be made; however, this comparison is more ambiguous because of the presence of multiple SOA precursors and contributions from primary aerosols. Nevertheless, the O:C value of 0.83 falls in between that of urban "fresh" organic aerosol (OA) (0.52−0.64) and urban "aged" OA (0.8 −1.02)[43] measured in Mexico City.

3.2. Organic Nitrogen in the Aerosol Phase. A significant fraction of SOA compounds formed under high-NO_x conditions are NOC species. Figure 3 shows the distribution of assigned molecules containing zero-, one-, two- and three-nitrogen atoms. Approximately 33% (by count) of all peaks in the high-NO_x mass spectrum are assigned to NOC, with 27% containing one, 5% containing two, and less than 1% containing three nitrogen atoms. In the high-NO_x sample, the smallest NOC molecule detected by (−) ESI-MS is the nitrate ester of 2-methylglyceric acid (2MGA nitrate, henceforth). In contrast, only 1% of peaks are assigned to NOC in the low-NO_x samples; they likely result from the reactions of the residual NO (<1 ppb).

Figure S3 and Table S2 in the SI section shows the high resolution MS^n data for selected NOC species observed in this work. A distinct CID (collision induced dissociation) pattern confirms the identity of NOC in high-NO_x isoprene SOA as hydroxy organic nitrates based on the even-electron losses of

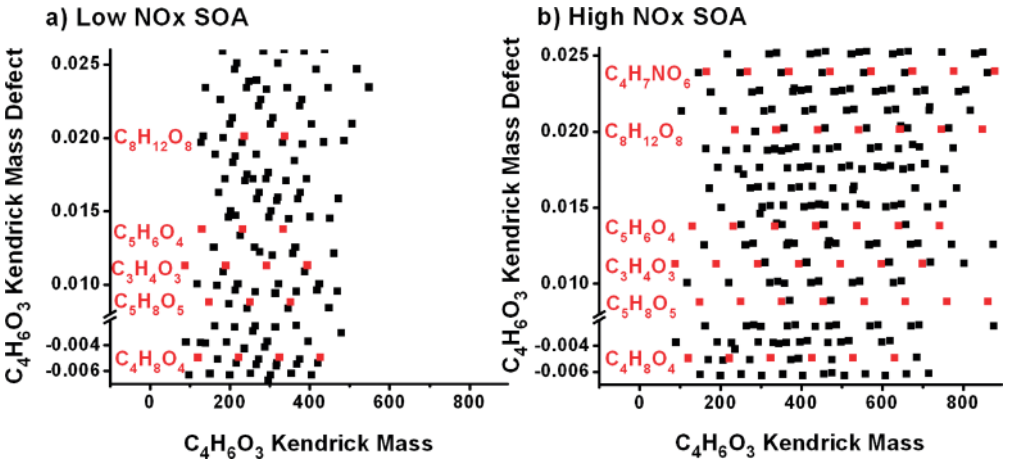

Figure 4. Magnified view of the $C_4H_6O_3$ Kendrick diagram for SOA obtained from photooxidation of isoprene under (a) low NO_x and (b) high NO_x conditions. Homologous series differing in repetitive $C_4H_6O_3$ units fall on the same horizontal lines with identical Kendrick mass defects. Selected families are shown in red to highlight especially long homologous series of 2MGA esters.

62.996 Da (HNO_3) and 77.011 Da (CH_3NO_3).[8] This fragmentation pattern is shown for a representative molecular ion $C_{13}H_{20}NO_{13}^-$ in SI Figure S3. Consistent with previous observations, most of the organic nitrates are derived from 2MGA oligomer esters.[8,23,44] Additionally, a neutral fragment corresponding to the dehydrated nitrate ester of a 2-methyltetrol ($C_5H_{11}NO_6$) was also inferred from the CID spectra as a loss of 163.047 Da ($C_5H_9NO_5$). This CID pattern suggests that 2-methyltetrol nitrates are produced in the high-NO_x photooxidation and are incorporated into the SOA constituents through oligomerization. Different fragmentation patterns would be observed if the NOC compounds contained nitro groups (—NO_2), nitrites (—ONO), aliphatic amines (—NH—), imines (=N—) or *N*-heterocyclic compounds.[45−47]

In addition to the losses of N-containing fragments, loss of 102.032 Da ($C_4H_6O_3$) is the most common neutral loss for all NOC oligomers observed in MS^n experiments. Based on the present observation of product ions and previous work by Surratt et al. (2006), the $C_4H_6O_3$ neutral loss is used as a signature of 2MGA-based esters. However, it is important to note that $C_4H_6O_3$ is not unique to either isoprene SOA oligomers or to aliphatic esters in general. $C_4H_6O_3$ fragment has been also observed in the MS^n spectra of fused sugar rings [48−52] that are structurally different than the 2MGA oligomerization products. The MS^n fragment ions produced from CID of selected peaks are listed in Supporting Information Table S2; examples include m/z 119.035 Da ($C_4H_7O_4^-$, deprotonated 2MGA), 189.040 Da ($C_7H_9O_6^-$, deprotonated 2MGA+ pyruvic acid), and 164.0198 Da ($C_4H_6NO_6^-$, deprotonated 2MGA nitrate).

The incorporation of —ONO_2 groups in 33% of the compounds contributes to the increased O:C ratio in the high-NO_x data (Figure 2). The majority of the NOC have more than 10 C-atoms, and even large (C > 20) compounds have just one nitrate group. As a result, the intensity-weighted average N:C ratio in high-NO_x SOA is relatively low (0.019). This value is comparable to the N:C ratio of ambient OA measured by AMS both in Mexico City (~0.02) [43]—a site dominated by urban OA, and on Whistler Mountain, Canada (~0.03) [42]—a site affected by both biogenic and anthropogenic emissions.

In the atmosphere, the NOC fraction in $PM_{2.5}$ is significant.[53−55] More than 20% of the particulate mass observed in Atlanta, Georgia, a site with high isoprene mixing ratios, is attributed to organic nitrates based on single particle mass spectrometry.[56] Our results underscore the importance of isoprene photooxidation as a source of atmospheric NOC. The mixing ratio of isoprene in an urban atmosphere can range from 2 ppb[57] to 6 ppb.[58] An SOA mass yield of 3% from the photooxidation of isoprene [2,15] will produce an estimated 0.08−0.25 $\mu g/m^3$ aerosol mass. Therefore, a 33% organic nitrate yield from our work, applied to the 0.08−0.25 $\mu g/m^3$ aerosol mass estimated from isoprene, corresponds to 0.03−0.08 $\mu g/m^3$ of particulate organic nitrates in the atmosphere. For comparison, the total airborne particulate organic nitrate mass measured in the afternoon in Pasadena, CA is 0.12 $\mu g/m^3$.[59] The above estimation suggests that a substantial fraction (30−70%) of these nitrates may come from isoprene. We note, however, that the contribution of isoprene loading in Pasadena, CA is much less than anthropogenic VOC loading.

3.3. Oligomer Building Blocks. A unique aspect of (−) ESI-MS is the soft ionization of very large oligomers. MS^n studies (Section 3.2) confirmed that these oligomers are covalently bound molecules (as opposed to ionic clusters that may be occasionally formed in ESI) as evidenced by the high CID threshold energy necessary for fragmentation. Under our normal experimental conditions, the ionic clusters, even when they are formed in the ESI source, do not survive the transfer from the LTQ to the Orbitrap. All major peaks in the mass-spectra shown in Figure 1 correspond to deprotonated molecular ions. Oligomer esters of 2MGA [8,22,23] appear in the mass spectra as families of peaks differing in mass units of 102.032 Da ($C_4H_6O_3$ - dehydrated 2MGA). The long homologous chemical families found in isoprene SOA are best showcased with a Kendrick analysis,[29,60,61] where the masses of the observed compounds are renormalized from a ^{12}C-based mass adopted by the IUPAC system to another base commonly repeated in the mass spectra, e.g. by setting the mass of $C_4H_6O_3$ to the integer value of 102 Da. The renormalized masses are now termed the $C_4H_6O_3$ Kendrick mass (KM) and the difference between the KM and the nominal mass is termed the Kendrick mass defect (KMD). Homologous series of peaks differing in one $C_4H_6O_3$ unit, arising from repetitive incorporation of the monomer 2MGA will have identical values of KMD. An assignment of any

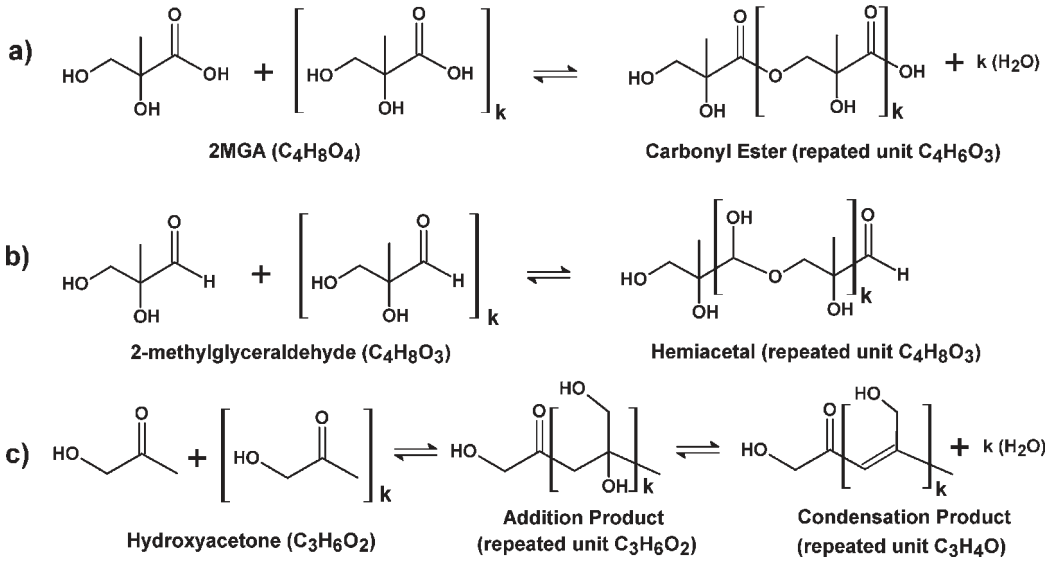

Figure 5. Illustrative examples of self-oligomerization reactions of (a) 2-methylglyceric acid (2MGA) producing carbonyl esters through condensation chemistry from repeated integration of $C_4H_6O_3$ units (b) 2-methylglyceraldehyde producing linear hemiacetals through addition chemistry from repeated integration of $C_4H_8O_3$ units and (c) hydroxyacetone producing an aldol through addition chemistry from repeated integration of $C_3H_6O_2$ units, followed by the formation of an aldol condensation product via loss of H_2O, which results in repeated C_3H_4O units.

member in the series is sufficient for assigning molecular formulas to the remaining homologous peaks.

Figure 4 shows a $C_4H_6O_3$-based Kendrick diagram of isoprene SOA formed under high- and low-NO_x conditions. Based on the KMD analysis, important molecules that produce long oligomer ester series with 2MGA are $C_3H_4O_3$ (pyruvic acid), $C_4H_8O_3$, $C_4H_8O_4$ (2MGA), $C_4H_7NO_6$ (2MGA nitrate), $C_5H_6O_4$, $C_5H_8O_5$, $C_6H_{10}O_5$, and $C_8H_{12}O_8$ (likely a hemiacetal dimer of 2MGA). The lines shown in red correspond to the longest observed homologous series, including the 2MGA nitrates ($C_4H_7NO_6$+ $(C_4H_6O_3)_{[0-3]}$) reported by Surratt et al. (2006) for high-NO_x SOA. Some of the observed NOC oligomers include up to 8 units of $C_4H_6O_3$ in high-NO_x SOA. In combination, the 2MGA-based NOC oligomers contribute significantly to the overall signal (~7% in combined peak abundance). In comparison, the contribution of the most prominent non-NOC family of 2MGA oligomer esters ($C_4H_8O_4$+ $(C_4H_6O_3)_{[0-6]}$) is about ~5%. Figure 4 also illustrates that the lengths of both NOC and nitrogen free oligomer series are shorter in low-NO_x SOA. For example, for the $C_5H_8O_5$+ $(C_4H_6O_3)_n$ series, n ranged up to 7 and the oligomers with n = 2,3 were the most abundant in the high-NO_x mass spectra. For the same series in the low-NO_x case, the oligomers with n = 0, 1 were the most abundant, and the longest observed oligomer corresponded to n = 2.

We performed a mass difference analysis to sift through the distributions of peaks and identify oligomeric units of primary importance in SOA growth reactions. In our previous study, we demonstrated that isoprene photooxidation SOA generated under two relative humidity conditions had different prevailing mass differences in the spectra: under dry conditions, 102.032 Da ($C_4H_6O_3$) was the most prominent mass difference from the prevalence of 2MGA oligomer esters, and under humid conditions 15.995 Da (O-atom) was the most prominent mass difference,[30,62] which is consistent with observations of Zhang et al. (2011).[62] Because we are interested in multifunctional oligomer building units, we limit our mass difference analysis to units containing at least two carbon atoms. We have examined all bases of the type $C_{(2-10)}H_{(2-20)}O_{(0-10)}$ using both the mass difference analysis (to find the most common mass differences) and Kendrick analysis (to identify the most prominent chemical families). Nitrogen was not included in the analysis for ease of comparison between the high-NO_x and low-NO_x data and because of the low N:C ratio for majority of SOA molecules. The resulting bases were considered as oligomer building blocks if they corresponded to an expected stable isoprene oxidation product capable of undergoing condensation or addition reactions resulting in the formation of oligomers.[8,63−68] Important condensation reactions include esterification, aldol condensation, and anhydride formation, and important addition reactions include hemiacetal formation, oxidative ring-opening, and related reactions. Condensation reactions between two monomers (M and M′) produce molecular formulas of the type (M + M′ − H_2O) and addition reactions produce molecular formulas of the type (M + M′). With addition reactions, the oligomer building block and the corresponding monomer are the same. Illustrative examples of such reactions are shown in Figure 5.

The three most important oligomer building blocks and the corresponding monomers, sorted by their frequency of occurrence in the mass spectra, are shown in Table 1. The high-NO_x data is divided into two NOC and nitrogen-free components. There is a significant degree of overlap between the oligomer building blocks found in each type of SOA. However, the frequencies of occurrence for the building blocks are different. The most prominent monomeric building blocks in the low-NO_x sample are smaller in size than those found in the high-NO_x sample. In the low-NO_x sample, the top two monomers are C_2 compounds derived from aldehydes, whereas in the high-NO_x sample, the top two monomers are C_3-C_4 compounds derived from organic acids. It appears that low-NO_x conditions generally favor the production of aldehydes and polyols leading to the dominance of addition-type oligomerization in aerosol, and high-NO_x conditions favor the production of multifunctional acids making the condensation-type chemistry more important.[8]

Table 1. Three Most Abundant Repeating Units in Isoprene Photooxidation SOA, Ranked by the Frequency of Their Occurrence in the Mass Spectra[a]

High-NOx Sample

Repeating Units	Frequency	Monomer	Monomer Name	Proposed Structure	Ref.
		NOC			
$C_4H_6O_3$ and $C_4H_8O_4$	204	$C_4H_8O_4$	2-methylglyceric acid (2MGA)	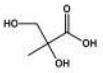	[6, 8, 23]
$C_3H_4O_2$	178	$C_3H_6O_3$ or $C_3H_4O_2$	lactic acid or methylglyoxal	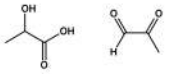	[67, 83-85]
C_2H_2O and $C_2H_4O_2$	174	$C_2H_4O_2$	glycolaldehyde		[78, 80, 86]
		Nitrogen free			
$C_3H_4O_2$	369	$C_3H_6O_3$ or $C_3H_4O_2$	lactic acid or methylglyoxal	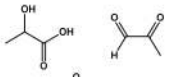	[67, 83-85]
$C_4H_6O_3$ and $C_4H_8O_4$	368	$C_4H_8O_4$	2-methylglyceric acid (2MGA)	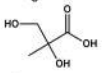	[6, 8, 23]
C_2H_4O	350	$C_2H_6O_2$ or C_2H_4O	acetaldehyde or ethylene glycol	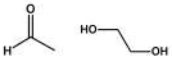	[82]

Low-NOx Sample

Repeating Units	Frequency	Monomer	Monomer Name	Proposed Structure	Ref.
		Nitrogen free			
C_2H_4O	438	$C_2H_6O_2$ or C_2H_4O	acetaldehyde or ethylene glycol	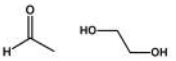	[82]
C_2H_2O and $C_2H_4O_2$	417	$C_2H_4O_2$	glycolaldehyde		[78, 80, 86]
C_3H_4O and $C_3H_6O_2$	404	$C_3H_6O_2$	hydroxyacetone		[78, 87]

[a] In the high-NO_x case, two separate rankings are provided for the NOC and non-NOC compounds. Literature references refer to observation of these monomers amongst products of isoprene photooxidation.

A more complete list of important oligomer building blocks inferred from the high-resolution (−) ESI-MS data is shown in Table S1 of the SI. As expected, all the monomers shown in Table 1 and SI Table S1 represent multifunctional compounds capable of self- or cross-oligomerization such as hydroxy carboxylic acids, keto carboxylic acids, or hydroxy carbonyls. The similarity in incorporation of oligomer building blocks between the low- and high-NO_x data may be due to similar low-volatility reaction products entering and reacting with each other in the aerosol phase and common heterogeneous uptake mechanisms (like reactive uptake of methylglyoxal).[69] Our analysis revealed several C_4-C_5 oligomer building blocks that are highly oxidized and functionalized but generally retain the carbon skeleton of isoprene. Larger monomers have low vapor pressure (e.g., the vapor pressure of 2MGA is estimated to be 4×10^{-5} Torr at 25 °C using the group contribution method by Pankow and Ascher[27]) and enter the particle-phase by physical condensation, after which, they partake in slow oligomerization reactions. It is likely that these molecules are not present in the monomeric form in particles due to their high reactivity.

Small (C_2-C_3) monomers in Table 1, which were observed in a number of isoprene oxidation studies as gas-phase products, are not expected to partition into the particle phase in their monomeric forms. They likely participate in oligomerization reactions through heterogeneous (surface) uptake. Heterogeneous reactions of glyoxal and methyglyoxal have been extensively investigated and their gas/particle partitioning is much greater than can be predicted based on their solubility in organic phase alone.[70−73] Methylglyoxal in particular, may contribute to organic particulate mass through reactions in weakly acidic instead of strongly acidic (e.g., sulfuric acid) media.[69] Our data, correspondingly, suggest that methylglyoxal is an important contributor to isoprene SOA growth.

The prevalence of the mass differences $C_2H_2O/C_2H_4O_2$, $C_2H_2O_2$, and $C_3H_6O_2$ between SOA individual constituents suggest that glycolaldehyde, hydroxyacetic acid, and hydroxyacetone, respectively, are also involved in oligomerization reactions either in the gas phase followed by gas-particle partitioning or by reactive uptake onto organic aerosols. These small carbonyl compounds are present in significant quantity in the isoprene + OH reaction.[26,74,75] Glycolaldehyde was also suggested by Lim et al. (2005) to be an important cloud-processing source of SOA through aqueous uptake.[76] However, uptake experiments of several carbonyl compounds on inorganic seed particles by Kroll et al. (2005) concluded that equilibrium partitioning and

acid-catalyzed uptake was not significant for methylglyoxal and hydroxyacetone.[72] The disagreement between the predictions derived from HR-MS with the observations by Kroll et al. (2005)[72] may be due to differences in surface reactions of these molecules on pre-existing SOA organics vs inorganic seed particles. In our experiments, inorganic seeds were not used and the aerosol particles were comprised entirely of organic material. Further investigation of heterogeneous reactions of methyglyoxal, glycolaldehyde, and hydroxyacetone on model aerosol surfaces is warranted because they are important isoprene photooxidation products.[75,77−82]

In summary, a wealth of molecular information, for example, formation of complex organic nitrates, distribution of functional groups in the molecules (from MS^n studies), insights into the mechanism of oligomer formation (from repeating units), can be extracted from the HR-MS data. The average elemental composition in the form of the O:C, H:C, and N:C ratios can also be extracted, and it is in good agreement with the information obtained by online methods such as AMS. However, such averaged quantities do not fully convey the heterogeneity of the molecular structures of the SOA compounds. Detailed molecular information provided by high-resolution mass spectrometry helps us better understand and predict the chemistry and physics of SOA, for example, , how molecules in SOA react with each other and with atmospheric radicals, how they absorb solar radiation, and how they interact with water vapor.

■ ASSOCIATED CONTENT

Supporting Information. Yields of selected VOC and SOA formed from photooxidation of isoprene under low-NO_x and high-NO_x conditions (Figure S1). Mixing ratios of the gas-phase products measured with PTR-ToF-MS. (Figure S2). Representative MS^n spectra of NOC oligomers (Figure S3). List of repeating oligomer units determined from mass difference analysis (Table S1). Table of MS^n fragmentation products of selected NOC oligomers (Table S2). This material is available free of charge via the Internet at http://pubs.acs.org.

■ AUTHOR INFORMATION

Corresponding Author

*Phone: 949-824-1262; e-mail: nizkorod@uci.edu.

■ ACKNOWLEDGMENT

The UCI group acknowledges support by the NSF grants ATM-0831518 and CHEM-0909227. The PNNL group acknowledges support from the Chemical Sciences Division, Office of Basic Energy Sciences of the U.S. DOE, and the intramural research and development program of the W.R. Wiley Environmental Molecular Sciences Laboratory (EMSL). EMSL is a national scientific user facility located at PNNL, and sponsored by the Office of Biological and Environmental Research of the U.S. PNNL is operated for US DOE by Battelle Memorial Institute under Contract No. DE-AC06-76RL0 1830.

■ REFERENCES

(1) Guenther, A.; Karl, T.; Harley, P.; Wiedinmyer, C.; Palmer, P. I.; Geron, C. Estimates of global terrestrial isoprene emissions using MEGAN (Model of Emissions of Gases and Aerosols from Nature). *Atmos. Chem. Phys.* **2006**, *6*, 3181–3210.

(2) Henze, D. K., Seinfeld, J. H.; , Global secondary organic aerosol from isoprene oxidation. *Geophys. Res. Lett.* **2006**, *33*, L09812, DOI: 10.1029/2006GL025976

(3) Heald, C. L.; Henze, D. K.; Horowitz, L. W.; Feddema, J.; Lamarque, J. F.; Guenther, A.; Hess, P. G.; Vitt, F.; Seinfeld, J. H.; Goldstein, A. H.; Fung, I., Predicted change in global secondary organic aerosol concentrations in response to future climate, emissions, and land use change. *J. Geophys. Res.-Atmos.* **2008**, *113*, (D5), D05211, DOI: 10.1029/2007jd009092.

(4) van Donkelaar, A.; Martin, R. V.; Park, R. J.; Heald, C. L.; Fu, T.-M.; Liao, H.; Guenther, A. Model evidence for a significant source of secondary organic aerosol from isoprene. *Atmos. Environ.* **2007**, *41* (6), 1267–1274.

(5) Claeys, M.; Graham, B.; Vas, G.; Wang, W.; Vermeylen, R.; Pashynska, V.; Cafmeyer, J.; Guyon, P.; Andreae, M. O.; Artaxo, P.; Maenhaut, W. Formation of secondary organic aerosols through photooxidation of isoprene. *Science* **2004**, *303* (5661), 1173–1176.

(6) Edney, E. O.; Kleindienst, T. E.; Jaoui, M.; Lewandowski, M.; Offenberg, J. H.; Wang, W.; Claeys, M. Formation of 2-methyl tetrols and 2-methylglyceric acid in secondary organic aerosol from laboratory irradiated isoprene/NO_x/SO_2/air mixtures and their detection in ambient $PM_{2.5}$ samples collected in the eastern United States. *Atmos. Environ.* **2005**, *39* (29), 5281–5289.

(7) Wang, W.; Kourtchev, I.; Graham, B.; Cafmeyer, J.; Maenhaut, W.; Claeys, M. Characterization of oxygenated derivatives of isoprene related to 2-methyltetrols in Amazonian aerosols using trimethylsilylation and gas chromatography/ion trap mass spectrometry. *Rapid Commun. Mass Spectrom.* **2005**, *19*, 1343–1351.

(8) Surratt, J. D.; Murphy, S. M.; Kroll, J. H.; Ng, N. L.; Hildebrandt, L.; Sorooshian, A.; Szmigielski, R.; Vermeylen, R.; Maenhaut, W.; Claeys, M.; Flagan, R. C.; Seinfeld, J. H. Chemical composition of secondary organic aerosol formed from the photooxidation of isoprene. *J. Phys. Chem. A* **2006**, *110* (31), 9665–9690.

(9) Jaoui, M.; Corse, E. W.; Lewandowski, M.; Offenberg, J. H.; Kleindienst, T. E.; Edney, E. O. Formation of organic tracers for isoprene SOA under acidic conditions. *Atmos. Environ.* **2010**, *44* (14), 1798–1805.

(10) Alves, C.; Gonçalves, C.; Mirante, F.; Nunes, T.; Evtyugina, M.; Sánchez de la Campa, A.; Rocha, A.; Marques, M. Organic speciation of atmospheric particles in Alvão Natural Park (Portugal). *Environ. Monit. Assess.* **2010**, *168* (1), 321–337.

(11) Dommen, J.; Metzger, A.; Duplissy, J.; Kalberer, M.; Alfarra, M. R.; Gascho, A.; Weingartner, E.; Prevot, A. S. H.; Verheggen, B.; Baltensperger, U., Laboratory observation of oligomers in the aerosol from isoprene/NO_x photooxidation. *Geophys. Res. Lett.* **2006**, *33*, (13), L13805, DOI: 10.1029/2006gl026523.

(12) Kalberer, M.; Sax, M.; Samburova, V. Molecular size evolution of oligomers in organic aerosols collected in urban atmospheres and generated in a smog chamber. *Environ. Sci. Technol.* **2006**, *40* (19), 5917–5922.

(13) Barket, D. J., Grossenbacher, J. W.; Hurst, J. M.; Shepson, P. B.; Olszyna, K.; Thornberry, T.; Carroll, M. A.; Roberts, J.; Stroud, C.; Bottenheim, J.; Biesenthal, T. A study of the NO_x dependence of isoprene oxidation. *J. Geophys. Res., [Atmos.]* **2004**, *109* (D11), D11310 (DOI: 10.1029/2003jd003965).

(14) Kroll J. H., N. L. N., Murphy, S. M.; Flagan, R. C.; , Seinfeld, J. H.; , Secondary organic aerosol formation from isoprene photooxidation under high-NO x conditions. *Geophys. Res. Lett.* **2005**, *32*, L18808, DOI: 10.1029/2005GL023637

(15) Kroll, J. H.; Ng, N. L.; Murphy, S. M.; Flagan, R. C.; Seinfeld, J. H. Secondary organic aerosol formation from isoprene photooxidation. *Environ. Sci. Technol.* **2006**, *40* (6), 1869–1877.

(16) Finlayson-Pitts, B. J.; Pitts, J. N., *Chemistry of the Upper and Lower Atmosphere: Theory, Experiments, and Applications*; Academic Press: San Diego, CA, 2000, ISBN10:012257060X.

(17) Tuazon, E. C.; Atkinson, R. A product study of the gas-phase reaction of isoprene with the OH radical in the presence of NO_x. *Int. J. Chem. Kinet.* **1990**, *22* (12), 1221–1236.

(18) Sprengnether, M.; Demerjian, K. L.; Donahue, N. M.; Anderson, J. G., Product analysis of the OH oxidation of isoprene and 1,3-

butadiene in the presence of NO. *J. Geophys. Res.* **2002**, *107*, (D15), 4268−4281, DOI: 10.1029/2001JD000716

(19) Paulot, F.; Crounse, J. D.; Kjaergaard, H. G.; Kroll, J. H.; Seinfeld, J. H.; Wennberg, P. O. Isoprene photooxidation: new insights into the production of acids and organic nitrates. *Atmos. Chem. Phys.* **2009**, *9*, 1479–1501.

(20) Werner, G.; Kastler, J.; Looser, R.; Ballschmiter, K. Organic nitrates of isoprene as atmospheric trace compounds. *Angew. Chem., Int. Ed.* **1999**, *38*, 1634–1637.

(21) Carlton, A. G.; Wiedinmyer, C.; Kroll, J. H. A review of secondary organic aerosol formation from isoprene. *Atmos. Chem. Phys.* **2009**, *9* (14), 4987–5005.

(22) Szmigielski, R.; Surratt, J. D.; Vermeylen, R.; Szmigielska, K.; Kroll, J. H.; Ng, N. L.; Murphy, S. M.; Sorooshian, A.; Seinfeld, J. H.; Claeys, M. Characterization of 2-methylglyceric acid oligomers in secondary organic aerosol formed from the photooxidation of isoprene using trimethylsilylation and gas chromatography/ion trap mass spectrometry. *J. Mass. Spectrom.* **2007**, *42* (1), 101–116.

(23) Chan, A. W. H.; Chan, M. N.; Surratt, J. D.; Chhabra, P. S.; Loza, C. L.; Crounse, J. D.; Yee, L. D.; Flagan, R. C.; Wennberg, P. O.; Seinfeld, J. H. Role of aldehyde chemistry and NO_x concentrations in secondary organic aerosol formation. *Atmos. Chem. Phys.* **2010**, *10*, 7169–7188.

(24) Zhao, J.; Zhang, R. Proton transfer reaction rate constants between hydronium ion (H_3O^+) and volatile organic compounds. *Atmos. Environ.* **2004**, *38* (14), 2177–2185.

(25) Aschmann, S. M.; Atkinson, R. Formation yields of methyl vinyl ketone and methacrolein from the gas-phase reaction of O_3 with isoprene. *Environ. Sci. Technol.* **1994**, *28* (8), 1539–1542.

(26) Tuazon, E. C.; Atkinson, R. A product study of the gas-phase reaction of methyl vinyl ketone with the OH radical in the presence of NO_x. *Int. J. Chem. Kinet.* **1989**, *21*, 1141–1152.

(27) Pankow, J. F.; Asher, W. E. SIMPOL.1: a simple group contribution method for predicting vapor pressures and enthalpies of vaporization of multifunctional organic compounds. *Atmos. Chem. Phys.* **2008**, *8*, 2773–2796.

(28) Ng, N. L.; Kwan, A. J.; Surratt, J. D.; Chan, A. W. H.; Chhabra, P. S.; Sorooshian, A.; Pye, H. O. T.; Crounse, J. D.; Wennberg, P. O.; Flagan, R. C.; Seinfeld, J. H. Secondary organic aerosol (SOA) formation from reaction of isoprene with nitrate radicals (NO_3). *Atmos. Chem. Phys.* **2008**, *8* (14), 4117–4140.

(29) Nguyen, T. B.; Bateman, A. P.; Bones, D. L.; Nizkorodov, S. A.; Laskin, J.; Laskin, A. High-resolution mass spectrometry analysis of secondary organic aerosol generated by ozonolysis of isoprene. *Atmos. Environ.* **2010**, *44* (8), 1032–1042.

(30) Nguyen, T. B.; Roach, P. J.; Laskin, J.; Laskin, A.; Nizkorodov, S. A. Effect of humidity on the composition and yield of isoprene photooxidation secondary organic aerosol. *Atm. Chem. Phys.* **2011**, *708* (11), 6931−6944 (DOI:10.5194/acp-11-6931-2011).

(31) van Krevelen, D. W. Graphical-statistical method for the study of structure and reaction processes of coal. *Fuel* **1950**, *29*, 269–84.

(32) Kim, S.; Kramer, R. W.; Hatcher, P. G. Graphical method for analysis of ultrahigh-resolution broadband mass spectra of natural organic matter, the van Krevelen diagram. *Anal. Chem.* **2003**, *75* (20), 5336–5344.

(33) Nash, D. G.; Baer, T.; Johnston, M. V. Aerosol mass spectrometry: An introductory review. *Int. J. Mass Spec.* **2006**, *258* (1−3), 2–12.

(34) Chhabra, P. S.; Flagan, R. C.; Seinfeld, J. H. Elemental analysis of chamber organic aerosol using an aerodyne high-resolution aerosol mass spectrometer. *Atmos. Chem. Phys.* **2010**, *10* (9), 4111–4131.

(35) Farmer, D. K.; Matsunaga, A.; Docherty, K. S.; Surratt, J. D.; Seinfeld, J. H.; Ziemann, P. J.; Jimenez, J. L. Response of an aerosol mass spectrometer to organonitrates and organosulfates and implications for atmospheric chemistry. *Proc. Natl. Acad. Sci.* **2010**, *107* (15), 6670–6675.

(36) Chen, Q.; Farmer, D. K.; Schneider, J.; Zorn, S. R.; Heald, C. L.; Karl, T. G.; Guenther, A.; Allan, J. D.; Robinson, N.; Coe, H.; Kimmel, J. R.; Pauliquevis, T.; Borrmann, S.; Pöschl, U.; Andreae, M. O.; Artaxo, P.; Jimenez, J. L.; Martin, S. T., Mass spectral characterization of submicron biogenic organic particles in the Amazon Basin. *Geophys. Res. Lett.* **2009**, *36*, (20), L20806, DOI: 10.1029/2009gl039880.

(37) Shilling, J. E.; Chen, Q.; King, S. M.; Rosenoern, T.; Kroll, J. H.; Worsnop, D. R.; DeCarlo, P. F.; Aiken, A. C.; Sueper, D.; Jimenez, J. L.; Martin, S. T. Loading-dependent elemental composition of alpha-pinene SOA particles. *Atmos. Chem. Phys.* **2009**, *9* (3), 771–782.

(38) Heaton, K. J.; Dreyfus, M. A.; Wang, S.; Johnston, M. V. Oligomers in the early stage of biogenic secondary organic aerosol formation and growth. *Environ. Sci. Technol.* **2007**, *41* (17), 6129–6136.

(39) Gao, Y.; Hall, W. A.; Johnston, M. V. Molecular composition of monoterpene secondary organic aerosol at low mass loading. *Environ. Sci. Technol.* **2010**, *44* (20), 7897–7902.

(40) Bateman, A. P.; Nizkorodov, S. A.; Laskin, J.; Laskin, A. Time-resolved molecular characterization of limonene/ozone aerosol using high-resolution electrospray ionization mass spectrometry. *Phys. Chem. Chem. Phys.* **2009**, *11* (36), 7931–7942.

(41) Walser, M. L.; Desyaterik, Y.; Laskin, J.; Laskin, A.; Nizkorodov, S. A. High-resolution mass spectrometric analysis of secondary organic aerosol produced by ozonation of limonene. *Phys. Chem. Chem. Phys.* **2008**, *10* (7), 1009–1022.

(42) Sun, Y.; Zhang, Q.; Macdonald, A. M.; Hayden, K.; Li, S. M.; Liggio, J.; Liu, P. S. K.; Anlauf, K. G.; Leaitch, W. R.; Steffen, A.; Cubison, M.; Worsnop, D. R.; van Donkelaar, A.; Martin, R. V. Size-resolved aerosol chemistry on Whistler Mountain, Canada with a high-resolution aerosol mass spectrometer during INTEX-B. *Atmos. Chem. Phys.* **2009**, *9* (9), 3095–3111.

(43) Aiken, A. C.; Decarlo, P. F.; Kroll, J. H.; Worsnop, D. R.; Huffman, J. A.; Docherty, K. S.; Ulbrich, I. M.; Mohr, C.; Kimmel, J. R.; Sueper, D.; Sun, Y.; Zhang, Q.; Trimborn, A.; Northway, M.; Ziemann, P. J.; Canagaratna, M. R.; Onasch, T. B.; Alfarra, M. R.; Prevot, A. S. H.; Dommen, J.; Duplissy, J.; Metzger, A.; Baltensperger, U.; Jimenez, J. L. O/C and OM/OC ratios of primary, secondary, and ambient organic aerosols with high-resolution time-of-flight aerosol mass spectrometry. *Environ. Sci. Technol.* **2008**, *42* (12), 4478–4485.

(44) Surratt, J.; Chan, A. W. H.; Eddingsaas, N. C.; Chan, M.; Loza, C. L.; Kwan, A. J.; Hersey, S. P.; Flagan, R. C.; Wennberg, P. O.; Seinfeld, J. H. Reactive intermediates revealed in secondary organic aerosol formation from isoprene. *Proc. Natl. Acad. Sci.* **2010**, *107*, 6640–6645.

(45) Reemtsma, T.; These, A.; Venkatachari, P.; Xia, X. Y.; Hopke, P. K.; Springer, A.; Linscheid, M. Identification of fulvic acids and sulfated and nitrated analogues in atmospheric aerosol by electrospray ionization Fourier transform ion cyclotron resonance mass spectrometry. *Anal. Chem.* **2006**, *78* (24), 8299–8304.

(46) Yinon, J.; McClellan, J. E.; Yost, R. A. Electrospray ionization tandem mass spectrometry collision-induced dissociation study of explosives in an ion trap mass spectrometer. *Rapid Commun. Mass Spectrom.* **1997**, *11* (18), 1961–1970.

(47) Levsen, K.; Schiebel, H. M.; Terlouw, J. K.; Jobst, K. J.; Elend, M.; Preib, A.; Thiele, H.; Ingendoh, A. Even-electron ions: a systematic study of the neutral species lost in the dissociation of quasi-molecular ions. *J. Mass. Spectrom.* **2007**, *42* (8), 1024–1044.

(48) Nunes, F. M.; Domingues, M. R.; Coimbra, M. A. Arabinosyl and glucosyl residues as structural features of acetylated galactomannans from green and roasted coffee infusions. *Carbohydr. Res.* **2005**, *340* (10), 1689–1698.

(49) Simoes, J.; Nunes, F. M.; Domingues, M. D. M.; Coimbra, M. A. Structural features of partially acetylated coffee galactomannans presenting immunostimulatory activity. *Carbohydr. Polym.* **2010**, *79* (2), 397–402.

(50) Quéméner, B.; Cabrera Pino, J. C.; Ralet, M.-C.; Bonnin, E.; Thibault, J.-F. Assignment of acetyl groups to O-2 and/or O-3 of pectic oligogalacturonides using negative electrospray ionization ion trap mass spectrometry. *J. Mass. Spectrom.* **2003**, *38* (6), 641–648.

(51) Ralet, M. C.; Cabrera, J. C.; Bonnin, E.; Quemener, B.; Hellin, P.; Thibault, J. F. Mapping sugar beet pectin acetylation pattern. *Phytochemistry* **2005**, *66* (15), 1832–1843.

(52) Madeira, P. J. A.; Rosa, A. M.; Xavier, N. M.; Rauter, A. P.; Florêncio, M. H. Electrospray ionization mass spectrometric analysis of

newly synthesized α,β-unsaturated γ-lactones fused to sugars. *Rapid Commun. Mass Spectrom.* **2010**, *24*, 1049–1058.

(53) Zhang, Q.; Anastasio, C.; Jimenez-Cruz, M., Water-soluble organic nitrogen in atmospheric fine particles (PM2.5) from northern California. *J. Geophys. Res.* **2002**, *107*, (D11), 4112, DOI: 10.1029/2001jd000870.

(54) Duan, F.; Liu, X.; He, K.; Dong, S. Measurements and characteristics of nitrogen-containing compounds in atmospheric particulate matter in Beijing, China. *Bull. Environ. Contam. Toxicol.* **2009**, *82* (3), 332–337.

(55) Lin, M.; Walker, J.; Geron, C.; Khlystov, A. Organic nitrogen in $PM_{2.5}$ aerosol at a forest site in the Southeast US. *Atmos. Chem. Phys.* **2010**, *10* (5), 2145–2157.

(56) Lee, S. H.; Murphy, D. M.; Thomson, D. S.; Middlebrook, A. M., Nitrate and oxidized organic ions in single particle mass spectra during the 1999 Atlanta Supersite Project. *J. Geophys. Res., [Atmos.]* **2003**, *108*, (D7), 8417-8425, DOI: 10.1029/2001jd001455.

(57) Apel, E. C., Riemer, D. D.; Hills, A.; Baugh, W.; Orlando, J.; Faloona, I.; Tan, D.; Brune, W.; Lamb, B.; Westberg, H.; Carroll, M. A.; Thornberry, T.; Geron, C. D. Measurement and interpretation of isoprene fluxes and isoprene, methacrolein, and methyl vinyl ketone mixing ratios at the PROPHET site during the 1998 Intensive. *J. Geophys. Res., [Atmos.]* **2002**, *107* (D3), 4034−4049 (DOI: 10.1029/2000jd000225).

(58) Roberts, J. M., Stroud, C. A.; Goldan, P. D.; Kuster, W. C.; Murphy, P. C.; Williams, E. J.; Hereid, D.; Parrish, D.; Sueper, D.; Trainer, M.; Fehsenfeld, F. C.; Apel, E. C.; Riemer, D.; Wert, B.; Henry, B.; Fried, A.; Martinez-Harder, M.; Harder, H.; Brune, W. H.; Li, G.; Xie, H.; Young, V. L. Isoprene and its oxidation products, methacrolein and methylvinyl ketone, at an urban forested site during the 1999 Southern Oxidants Study. *J. Geophys. Res.* **2001**, *106* (D8), 8035−8046 (DOI:10.1029/2000jd900628).

(59) Novakov, T.; Mueller, P. K.; Alcocer, A. E.; Otvos, J. W. Chemical composition of Pasadena aerosol by particle size and time of day. III. Chemical states of nitrogen and sulfur by photoelectron spectroscopy. *J. Colloid Interface Sci.* **1972**, *39* (1), 225–234.

(60) Kendrick, E. Mass scale based on CH_2 = 14.0000 for high-resolution mass spectrometry of organic compounds. *Anal. Chem.* **1963**, *35* (13), 2146–54.

(61) Hughey, C. A.; Rodgers, R. P.; Marshall, A. G. Resolution of 11,000 compositionally distinct components in a single electrospray ionization fourier transform ion cyclotron resonance Mass spectrum of crude oil. *Anal. Chem.* **2002**, *74* (16), 4145–4149.

(62) Zhang, H.; Surratt, J. D.; Lin, Y. H.; Bapat, J.; Kamens, R. M. Effect of relative humidity on SOA formation from isoprene/NO photooxidation: role of particle-phase esterification under dry conditions. *Atmos. Chem. Phys. Discuss.* **2011**, *11*, 5407–5433.

(63) Hamilton, J. F.; Lewis, A. C.; Carey, T. J.; Wenger, J. C. Characterization of polar compounds and oligomers in secondary organic aerosol using liquid chromatography coupled to mass spectrometry. *Anal. Chem.* **2008**, *80* (2), 474–480.

(64) Barsanti, K. C.; Pankow, J. F. Thermodynamics of the formation of atmospheric organic particulate matter by accretion reactions—Part 1: aldehydes and ketones. *Atmos. Environ.* **2004**, *38* (26), 4371–4382.

(65) Barsanti, K. C.; Pankow, J. F. Thermodynamics of the formation of atmospheric organic particulate matter by accretion reactions—2. Dialdehydes, methylglyoxal, and diketones. *Atmos. Environ.* **2005**, *39* (35), 6597–6607.

(66) Barsanti, K. C.; Pankow, J. F. Thermodynamics of the formation of atmospheric organic particulate matter by accretion reactions—Part 3: Carboxylic and dicarboxylic acids. *Atmos. Environ.* **2006**, *40* (34), 6676–6686.

(67) Altieri, K. E.; Seitzinger, S. P.; Carlton, A. G.; Turpin, B. J.; Klein, G. C.; Marshall, A. G. Oligomers formed through in-cloud methylglyoxal reactions: Chemical composition, properties, and mechanisms investigated by ultra-high resolution FT-ICR mass spectrometry. *Atmos. Environ.* **2008**, *42* (7), 1476–1490.

(68) Noziere, B.; Esteve, W. Light-absorbing aldol condensation products in acidic aerosols: Spectra, kinetics, and contribution to the absorption index. *Atmos. Environ.* **2007**, *41* (6), 1150–1163.

(69) Zhao, J.; Levitt, N. P.; Zhang, R.; Chen, J. Heterogeneous reactions of methylglyoxal in acidic media: implications for secondary organic aerosol formation. *Environ. Sci. Technol.* **2006**, *40* (24), 7682–7687.

(70) Healy, R. M.; Wenger, J. C.; Metzger, A.; Duplissy, J.; Kalberer, M.; Dommen, J. Gas/particle partitioning of carbonyls in the photooxidation of isoprene and 1,3,5-trimethylbenzene. *Atmos. Chem. Phys.* **2008**, *8* (12), 3215–3230.

(71) Liggio, J.; Li, S.-M.; McLaren, R. Heterogeneous reactions of glyoxal on particulate matter: identification of acetals and sulfate esters. *Environ. Sci. Technol.* **2005**, *39* (6), 1532–1541.

(72) Kroll, J. H.; Ng, N. L.; Murphy, S. M.; Varutbangkul, V.; Flagan, R. C.; Seinfeld, J. H., Chamber studies of secondary organic aerosol growth by reactive uptake of simple carbonyl compounds. *J. Geophys. Res.* **2005**, *110*, (D23), D23207, DOI: 10.1029/2005JD006004

(73) Corrigan, A. L.; Hanley, S. W.; Haan, D. O. Uptake of glyoxal by organic and inorganic aerosol. *Environ. Sci. Technol.* **2008**, *42* (12), 4428–4433.

(74) Atkinson, R.; Arey, J. Atmospheric chemistry of biogenic organic compounds. *Acc. Chem. Res.* **1998**, *31* (9), 574–583.

(75) Williams, J.; Poschl, U.; Crutzen, P. J.; Hansel, A.; Holzinger, R.; Warneke, C.; Lindinger, W.; Lelieveld, J. An atmospheric chemistry interpretation of mass scans obtained from a proton transfer mass spectrometer flown over the tropical rainforest of Surinam. *J. Atmos. Chem.* **2001**, *38* (2), 133–166.

(76) Lim, H. J.; Carlton, A. G.; Turpin, B. J Isoprene forms secondary organic aerosol through cloud processing: model simulations. *Environ. Sci. Technol.* **2005**, *39*, 4441–4446.

(77) Moortgat, G. K.; Grossmann, D.; Boddenberg, A.; Dallmann, G.; Ligon, A. P.; Turner, W. V.; Gaeb, S.; Slemr, F.; Wieprecht, W.; Acker, K.; Kibler, M.; Schlomski, S.; Baechmann, K. Hydrogen peroxide, organic peroxides and higher carbonyl compounds determined during the BERLIOZ campaign. *J. Atmos. Chem.* **2002**, *42* (1−3), 443–463.

(78) Matsunaga, S. N.; Wiedinmyer, C.; Guenther, A. B.; Orlando, J. J.; Karl, T.; Toohey, D. W.; Greenberg, J. P.; Kajii, Y. Isoprene oxidation products are a significant atmospheric aerosol component. *Atmos. Chem. Phys. Discuss.* **2005**, *5*, 11143–11156.

(79) Lee, Y. N.; Zhou, X.; Kleinman, L. I.; Nunnermacker, L. J.; Springston, S. R.; Daum, P. H.; Newman, L.; Keigley, W. G.; Holdren, M. W.; Spicer, C. W.; Young, V.; Fu, B.; Parrish, D. D.; Holloway, J.; Williams, J.; Roberts, J. M.; Ryerson, T. B.; Fehsenfeld, F. C., Atmospheric chemistry and distribution of formaldehyde and several multioxygenated carbonyl compounds during the 1995 Nashville/Middle Tennessee Ozone Study. *J. Geophys. Res.* **1998**, *103*, (D17), 22449-22462, DOI: 10.1029/98jd01251.

(80) Spaulding, R. S.; Schade, G. W.; Goldstein, A. H.; Charles, M. J., Characterization of secondary atmospheric photooxidation products: Evidence for biogenic and anthropogenic sources. *J. Geophys. Res.* **2003**, *108*, (D8), 4247, DOI: 10.1029/2002jd002478.

(81) Zhou, X.; Huang, G.; Civerolo, K.; Schwab, J. Measurement of atmospheric hydroxyacetone, glycolaldehyde, and formaldehyde. *Environ. Sci. Technol.* **2009**, *43* (8), 2753–2759.

(82) Matsunaga, S.; Mochida, M.; Kawamura, K. Growth of organic aerosols by biogenic semi-volatile carbonyls in the forestal atmosphere. *Atmos. Environ.* **2003**, *37* (15), 2045–2050.

(83) Carlton, A. G.; Turpin, B. J.; Lim, H. J.; Altieri, K. E.; Seitzinger, S., Link between isoprene and secondary organic aerosol (SOA): Pyruvic acid oxidation yields low volatility organic acids in clouds. *Geophys. Res. Lett.* **2006**, *33*, (6), L06822, DOI: 10.1029/2005gl025374.

(84) Lim, Y. B.; Ziemann, P. J. Products and mechanism of secondary organic aerosol formation from reactions of n-alkanes with OH radicals in the presence of NO_x. *Environ. Sci. Technol.* **2005**, *39* (23), 9229–9236.

(85) Warneck, P. Multi-phase chemistry of C_2 and C_3 organic compounds in the marine atmosphere. *J. Atmos. Chem.* **2005**, *51* (2), 119–159.

(86) Lee, A.; Goldstein, A. H.; Kroll, J. H.; Ng, N. L.; Varutbangkul, V.; Flagan, R. C.; Seinfeld, J. H., Gas-phase products and secondary aerosol yields from the photooxidation of 16 different terpenes. *J. Geophys. Res.* **2006**, *111*, (D17), D17305, DOI: 10.1029/2006jd007050.

(87) Grosjean, D.; Williams, E. L.; Grosjean, E. Atmospheric chemistry of isoprene and of its carbonyl products. *Environ. Sci. Technol.* **1993**, *27* (5), 830–840.